

Control of Wing-Rock Motion of Slender Delta Wings

Jia Luo* and C. Edward Lan†
University of Kansas, Lawrence, Kansas 66045

A theoretical analysis is conducted to determine the optimal control input for wing-rock suppression through a Hamiltonian formulation. The optimality equations are analyzed through Beecham-Titchener's averaging technique and numerically integrated by a backward-differentiation formulas method developed for implicit differential equations. The weighting factors in the cost function are shown to be related explicitly to the system output damping and frequency. A numerical model constructed for an 80-deg delta wing is solved to illustrate the results. It is shown that Beecham-Titchener's technique is accurate in determining the necessary control function to suppress wing rock. From the numerical results, it is also shown that an effective way to suppress wing rock is to control the roll rate. System sensitivity is investigated by determining variations in system output damping and frequency with aerodynamic model coefficients. The results show that higher sensitivity corresponds to lower system damping.

Nomenclature

$a(t)$	= amplitude function
b	= wing span, ft
b_1, b_2, b_3	= weighting factors in J
d_{11}	$= \omega^2 - \mu^2 + c_1 - c_2\mu - \frac{8}{\pi} ac_4\mu\omega$
d_{12}	$= 2\mu\omega + c_2\omega + \frac{4}{3\pi} ac_3\omega + \frac{8}{3\pi} ac_4(\mu^2 + \omega^2)$
d_{21}	$= -2\mu\omega - c_2\omega - \frac{8}{3\pi} ac_3\omega + \frac{8}{3\pi} ac_4(\mu^2 - 2\omega^2)$
d_{22}	$= \omega^2 - \mu^2 + c_1 - c_2\mu$
h_1	$= 2\mu\omega - c_2\omega - \frac{4}{3\pi} c_3a\omega - \frac{4}{3\pi} c_4a(\mu^2 + 2\omega^2)$
h_2	$= \omega^2 - \mu^2 + c_1 + c_2\mu + \frac{8}{3\pi} c_3a\mu + \frac{8}{3\pi} c_4a\mu\omega$
H	= Hamiltonian defined in Eq. (5)
I_{xx}	= roll moment of inertia, slug-ft ²
J	= cost function defined in Eq. (4)
k_i	= feedback gains defined in Eq. (56)
L_0	$= qSbC_{l0}/I_{xx}, s^{-2}$
L_β	$= qSbC_{l\beta}/I_{xx}, s^{-2}$
L_{p0}	$= qSb^2C_{lp0}/(2I_{xx}V), s^{-1}$
$L_{p\beta}$	$= qSb^2C_{lp\beta}/(2I_{xx}V), s^{-1}$
L_{pp}	$= qSb^3C_{lpp}/(4I_{xx}V^2)$
p	= roll rate, rad/s
q	= dynamic pressure, lb/ft ²
S	= wing reference area, ft ²
u	= control function, rad/s ²
V	= freestream velocity, ft/s
ξ, η	= ratios of amplitude functions [Eqs. (11,12)]
λ_1, λ_2	= Lagrangian multipliers
μ	$= \dot{a}/a$
ω	$= \dot{\theta}$
ϕ	= bank angle, deg
$\theta(t)$	= phase function

Introduction

WING rock is a concern for combat aircraft because it may have adverse effects on maneuverability, tracking accuracy, and operational safety. Typically, it occurs at a moderate to high angle of attack and involves mainly the roll

degree of freedom. Recently, the phenomenon has received considerable attention among researchers. Experiments have been conducted on simple delta wings to help understand the fundamental mechanisms causing wing rock.^{1,2} Based on these test results, mathematical models for motion predictions have been proposed.^{3,4} In Ref. 3, models for both one-degree-of-freedom (DOF) and three-DOF motions were developed. In Ref. 4, only one-DOF models were considered. In Ref. 4, it was also indicated that to predict roll divergence, a cubic term in roll angle was needed in representing the rolling moment. In all these investigations, no control of the motion was considered.

Since wing rock is a nonlinear phenomenon, a method of analysis based on overall or local linearization is not appropriate. In Refs. 4 and 5, the analysis was based on a method of multiple time scales. Beecham-Titchener's (B-T) averaging technique⁶ was used in Ref. 3 to predict the limit-cycle frequency and amplitude of wing rock. The B-T method is a method of harmonic averaging that splits an equation into an in-phase part for the frequency and an out-of-phase one for the amplitude. To determine the necessary control for wing-rock suppression, the method of multiple time scales⁷ can be used. However, the B-T method will be used in the present analysis.

The main objective of this paper is to add a control function to the equation of wing-rock motion and to develop expressions showing the necessary control to suppress the motion using a Hamiltonian formulation. The resulting equations are solved by the B-T method. Since roll divergence is not considered, the one-DOF model of Ref. 3 will be employed to illustrate the concept. A specific numerical model of one DOF developed in Ref. 8, which is similar to that in Ref. 3, will be solved to demonstrate the results. Although only one DOF equation will be considered here, the B-T method is applicable to a system of nonlinear equations.⁹

Theoretical Development

Formulation of Equations

Consider the following one-DOF differential equation for wing-rock motion³:

$$\ddot{\phi} = L_0 + \sin \alpha_s L_\beta \phi + L_{p0} \dot{\phi} + \sin \alpha_s L_{p\beta} |\phi| \dot{\phi} + L_{pp} |\dot{\phi}| \dot{\phi} + u \quad (1)$$

where ϕ is the roll angle, α_s the steady angle of attack, and u the control function. Defining

$$c_0 = L_0, \quad c_1 = \sin \alpha_s L_\beta, \quad c_2 = L_{p0} \\ c_3 = \sin \alpha_s L_{p\beta}, \quad c_4 = L_{pp}$$

Received Sept. 3, 1991; revision received April 13, 1992; accepted for publication May 29, 1992. Copyright © 1992 by the American Institute of Aeronautics and Astronautics, Inc. All rights reserved.

*Graduate Research Assistant. Student Member AIAA.

†Professor, Aerospace Engineering and Center for Excellence in Computer Aided System Engineering. Associate Fellow AIAA.

we can rewrite Eq. (1) as

$$\dot{\phi} = p \quad (2)$$

$$\dot{p} = c_0 + c_1\phi + c_2p + c_3p\phi \operatorname{sgn}(\phi) + c_4p^2 \operatorname{sgn}(p) + u \quad (3)$$

where p is the roll rate. To suppress wing rock, a cost function is defined as

$$J = \int_0^T (b_1p^2 + b_2\phi^2 + b_3u^2) dt \quad (4)$$

in which the weighting factors satisfy

$$b_1 \geq 0, \quad b_2 \geq 0, \quad b_3 > 0$$

To minimize the cost function (4), the following Hamiltonian must be optimized:

$$H = b_1p^2 + b_2\phi^2 + b_3u^2 + \lambda_1p + \lambda_2[c_0 + c_1\phi + c_2p + c_3p\phi \operatorname{sgn}(\phi) + c_4p^2 \operatorname{sgn}(p) + u] \quad (5)$$

where λ_1 and λ_2 are the Lagrangian multipliers. The necessary optimality conditions are, in addition to Eqs. (2) and (3),

$$\dot{\lambda}_1 = -\partial H/\partial \phi = -2b_2\phi - \lambda_2c_1 - \lambda_2c_3p \operatorname{sgn}(\phi) \quad (6)$$

$$\begin{aligned} \dot{\lambda}_2 = -\partial H/\partial p = & -2b_1p - \lambda_1 - \lambda_2c_2 - \lambda_2c_3\phi \operatorname{sgn}(\phi) \\ & - 2\lambda_2c_4p \operatorname{sgn}(p) \end{aligned} \quad (7)$$

$$\partial H/\partial u = 2b_3u + \lambda_2 = 0 \quad (8)$$

From Eq. (8), the necessary control function can be obtained as

$$u = -\lambda_2/(2b_3) \quad (9)$$

One of the main problems in a direct integration of Eqs. (2–8) is that the conditions to be satisfied by λ_1 and λ_2 are specified at a large t , instead of $t=0^{10}$. To solve Eqs. (2), (3), (6), and (7) by the B-T method, let

$$\phi = a \cos \theta \quad (10)$$

$$\lambda_1 = a(\xi_1 \sin \theta + \eta_1 \cos \theta) \quad (11)$$

$$\lambda_2 = a(\xi_2 \sin \theta + \eta_2 \cos \theta) \quad (12)$$

where a , θ , ξ_1 , η_1 , ξ_2 , and η_2 are all functions of t . These specific forms for λ_1 and λ_2 are assumed because their solutions are expected to consist of an in-phase part (i.e., the $\cos \theta$ term) and an out-of-phase one (i.e., the $\sin \theta$ term) relative to $\phi(t)$. Differentiating Eqs. (10–12), we obtain

$$\dot{\phi} = a(\mu \cos \theta - \omega \sin \theta) \quad (13)$$

$$\ddot{\phi} = a \left\{ (\mu^2 - \omega^2 + a\mu\mu') \cos \theta - 2\mu\omega \left[1 + \frac{a(\omega^2)'}{4\omega^2} \right] \sin \theta \right\} \quad (14)$$

$$\dot{\lambda}_1 = a \left\{ [\mu(\xi_1 + a\xi_1') - \omega\eta_1] \sin \theta + [\mu(\eta_1 + a\eta_1') + \omega\xi_1] \cos \theta \right\} \quad (15)$$

$$\dot{\lambda}_2 = a \left\{ [\mu(\xi_2 + a\xi_2') - \omega\eta_2] \sin \theta + [\mu(\eta_2 + a\eta_2') + \omega\xi_2] \cos \theta \right\} \quad (16)$$

where

$$\mu = \dot{a}/a, \quad \omega = \dot{\theta}, \quad ()' = d()/da$$

For the first approximation, it is assumed that

$$\mu' = (\omega^2)' = \xi_1' = \eta_1' = \xi_2' = \eta_2' = 0$$

It follows that

$$\ddot{\phi} \approx a[(\mu^2 - \omega^2) \cos \theta - 2\mu\omega \sin \theta] \quad (17)$$

$$\dot{\lambda}_1 \approx a[(\mu\xi_1 - \omega\eta_1) \sin \theta + (\mu\eta_1 + \omega\xi_1) \cos \theta] \quad (18)$$

$$\dot{\lambda}_2 \approx a[(\mu\xi_2 - \omega\eta_2) \sin \theta + (\mu\eta_2 + \omega\xi_2) \cos \theta] \quad (19)$$

Assuming that a , μ , ω , ξ_1 , η_1 , ξ_2 , and η_2 do not change significantly over one oscillation cycle, substituting Eqs. (10–13) into Eqs. (1), (6), and (7), and integrating over one cycle

$$\int_0^{2\pi} (\text{Eq.}) \cos \theta d\theta, \quad \int_0^{2\pi} (\text{Eq.}) \sin \theta d\theta$$

we obtain

$$\mu^2 - \omega^2 = -\frac{\eta_2}{2b_3} + c_1 + c_2\mu + \frac{8}{3\pi}c_3a\mu + \frac{8}{3\pi}c_4a\mu\omega \quad (20)$$

$$2\mu\omega = \frac{\xi_2}{2b_3} + c_2\omega + \frac{4}{3\pi}c_3a\omega + \frac{4}{3\pi}c_4a(\mu^2 + 2\omega^2) \quad (21)$$

$$\mu\xi_1 - \omega\eta_1 = -c_1\xi_2 - \frac{4}{3\pi}ac_3(\mu\xi_2 - \omega\eta_2) \quad (22)$$

$$\mu\eta_1 + \omega\xi_1 = -2b_2 - c_1\eta_2 - \frac{8}{3\pi}ac_3\mu\eta_2 + \frac{4}{3\pi}ac_3\omega\xi_2 \quad (23)$$

$$\begin{aligned} \mu\xi_2 - \omega\eta_2 = & 2b_1\omega - \xi_1 - c_2\xi_2 - \frac{4}{3\pi}ac_3\xi_2 \\ & + \frac{8}{3\pi}ac_4(\mu\eta_2 - 2\omega\xi_2) \end{aligned} \quad (24)$$

$$\begin{aligned} \mu\eta_2 + \omega\xi_2 = & -2b_1\mu - \eta_1 - c_2\eta_2 - \frac{8}{3\pi}ac_3\eta_2 \\ & + \frac{8}{3\pi}ac_4(\mu\xi_2 - \omega\eta_2) \end{aligned} \quad (25)$$

Since both μ and ω contain first-order time derivatives, the B-T method basically splits a second-order equation (1) into two first-order equations [(20) and (21)]. One advantage of this method is that it shows clearly how the system damping, μ [Eq. (21)], is affected by the system parameters, such as c_2 , c_3 , and c_4 . To solve Eqs. (20) and (21) for μ and ω , ξ_2 and η_2 must be obtained first from Eqs. (22–25)

$$D \begin{bmatrix} \xi_2 \\ \eta_2 \end{bmatrix} = \begin{bmatrix} -4\mu\omega b_1 \\ 2(\mu^2 - \omega^2)b_1 - 2b_2 \end{bmatrix} \quad (26)$$

where D is a 2×2 matrix with elements d_{11} , d_{12} , d_{21} , and d_{22} defined in the nomenclature section. Equation (26) can be solved for ξ_2 and η_2 and these results are then substituted into Eqs. (20) and (21) to result in the equations for ω and μ . Alternatively, Eqs. (20) and (21) are solved for ξ_2/b_3 and η_2/b_3 , and these expressions are substituted into Eq. (26). The results are

$$-2\mu\omega(b_1/b_3) = d_{11}h_1 + d_{12}h_2 \quad (27a)$$

$$(\mu^2 - \omega^2)(b_1/b_3) - b_2/b_3 = d_{21}h_1 + d_{22}h_2 \quad (27b)$$

where h_1 and h_2 are defined in the nomenclature section.

Note that the λ_1 and λ_2 terms have been removed from the final equations (27). Since $\mu = \dot{a}/a$, $\omega = \dot{\theta}$, and b_1 , b_2 , b_3 are

constants, Eq. (27) represents an implicit differential equation of the form

$$F(y', y) = 0 \quad (28)$$

where F is a two-dimensional function and

$$y' = (\dot{a}, \dot{\theta})^T, \quad y = (a, \theta)^T$$

The present mathematical problem can therefore be summarized as follows. After specifying the weighting factors $b_1 - b_3$, Eq. (27) is integrated for $a(t)$ and $\theta(t)$. From Eqs. (20) and (21), ξ_2 and η_2 are then determined. Finally, the control function is obtained from Eq. (9). The weighting factors will be determined in the following way.

Equations (20) and (21) can be solved for μ and ω representing the damping and frequency of the nonlinear system. Since μ and ω do not change greatly according to the assumption of the B-T method, their initial values will be approximated with some desired values μ_d and ω_d , i.e.,

$$\mu(0) = \mu_d \quad (29)$$

$$\omega(0) = \omega_d \quad (30)$$

If the initial conditions of Eq. (1) are given as

$$\phi(0) = \phi_0 \quad (31)$$

$$\dot{\phi}(0) = \dot{\phi}_0 \quad (32)$$

then from Eqs. (1) and (13)

$$a_0 \cos \theta_0 = \phi_0$$

$$a_0(\mu_d \cos \theta_0 - \omega_d \sin \theta_0) = \dot{\phi}_0$$

from which θ_0 and a_0 can be obtained

$$\theta_0 = \tan^{-1} \frac{\mu_d \phi_0 - \dot{\phi}_0}{\omega_d \phi_0} \quad (33)$$

$$a_0 = \phi_0 / \cos \theta_0 \quad (34)$$

Using these initial values [Eqs. (29, 30, and 34)] in Eq. (27) and letting $b_3 = 1$, we can determine appropriate values for b_1 and b_2 . It is clear that for the present nonlinear system, the weighting factors b_1 and b_2 depend on the initial amplitude. However, for a linear system (i.e., $c_3 = c_4 = 0$), the matrix D and Eq. (27) are independent of a , and thus, b_1 and b_2 are independent of the initial amplitude a_0 .

Numerical Method of Integrating Eq. (27)

Equation (27) is an implicit differential equation and it cannot be solved analytically. For fully implicit ordinary differential equations, the approach of backward differentiation formulas (BDF) is an effective numerical method.¹¹ The code DASSL mentioned in Ref. 11 is used successfully to solve Eq. (27).

The implicit differential equation (28) with the initial conditions

$$y(t_0) = y_0 \quad (35)$$

$$y'(t_0) = y'_0 \quad (36)$$

must be compatible, i.e.,

$$F(y'_0, y_0) = 0 \quad (37)$$

In essence, the basic idea for finding the solution at t_{n+1} is to replace the time derivatives by backward differences and to

solve the resulting nonlinear algebraic equations by some variant of Newton's method. The specific algorithm of the present investigation uses both predictor and corrector formulas. At the predictor state, the solution at t_{n+1} is obtained by a predictor polynomial $g_{n+1}^p(t)$ that interpolates the previous solutions at the last $k + 1$ times

$$g_{n+1}^p(t_{n-i}) = y_{n-i}, \quad 0 \leq i \leq k \quad (38)$$

The interpolation method is based on divided differences. This predictor polynomial then provides the solution and its derivative at $t = t_{n+1}$

$$y_{n+1}^{(0)} = g_{n+1}^p(t_{n+1}) \quad (39)$$

$$y'_{n+1}^{(0)} = g'_{n+1}^p(t_{n+1}) \quad (40)$$

The final numerical solution at $t = t_{n+1}$ is the solution of a corrector polynomial $g_{n+1}^c(t)$ that interpolates the predictor

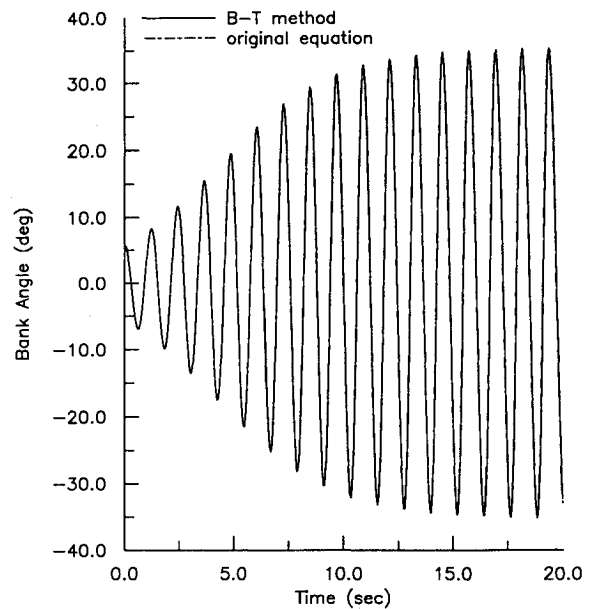


Fig. 1 Dynamic characteristics of wing rock based on Beecham-Titchener's method and numerical integration of the original equation.

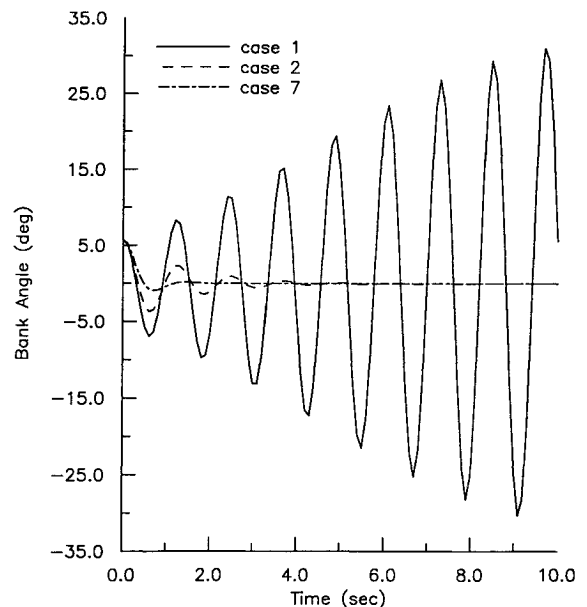


Fig. 2 Bank angle with and without control.

polynomial at k equally spaced points behind t_{n+1} and satisfies the original equation

$$g_{n+1}^c(t_{n+1}) = y_{n+1} \quad (41)$$

$$g_{n+1}^c(t_{n+1} - ih_{n+1}) = g_{n+1}^p(t_{n+1} - ih_{n+1}), \quad 1 \leq i \leq k \quad (42)$$

$$F[g_{n+1}^c(t_{n+1}), g_{n+1}^c(t_{n+1})] = 0 \quad (43)$$

Reference 12 suggests a method to find $g_{n+1}^c(t)$. Equation (42) implies that

$$g_{n+1}^c(t) - g_{n+1}^p(t) = b(t)[y_{n+1} - y_{n+1}^{(0)}] \quad (44)$$

where

$$\begin{aligned} b(t_{n+1} - ih_{n+1}) &= 0, & 1 \leq i \leq k \\ b(t_{n+1}) &= 1 \end{aligned} \quad (45)$$

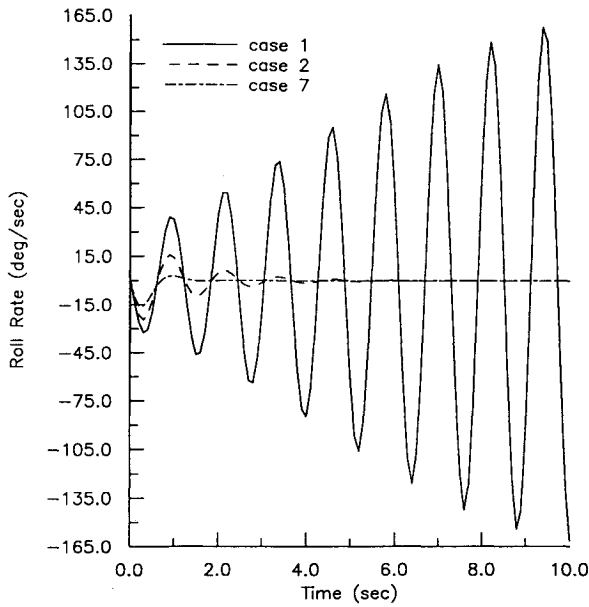


Fig. 3 Roll rate with and without control.

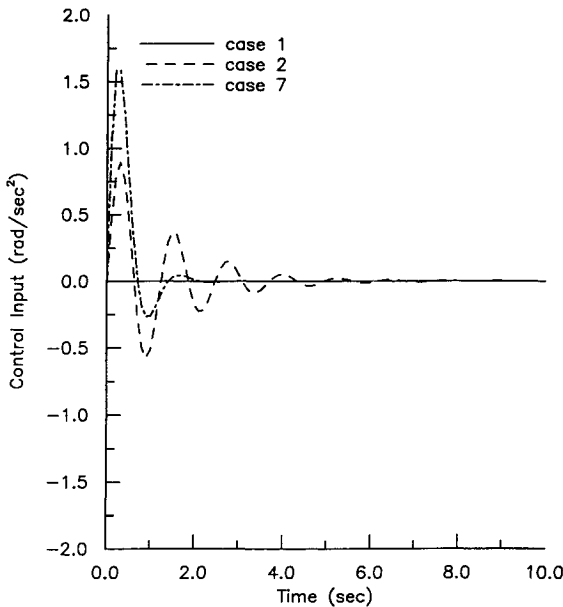


Fig. 4 Optimal control input.

With Eq. (45), the Lagrangian interpolation gives

$$b(t) = b(t_{n+1}) \cdot \frac{(t - t_{n+1} + kh_{n+1}) \cdots (t - t_{n+1} + h_{n+1})}{k! \cdot h_{n+1}^k} \quad (46)$$

and thus,

$$b'(t_{n+1}) = \frac{1}{h_{n+1}} \sum_{j=1}^k \frac{1}{j} \quad (47)$$

Differentiating Eq. (44) and letting $t = t_{n+1}$, we obtain

$$y'_{n+1} - y_{n+1}^{(0)} = b'(t_{n+1})[y_{n+1} - y_{n+1}^{(0)}] \quad (48)$$

from which y'_{n+1} can be determined. Substitution of y'_{n+1} into Eq. (28) gives

$$F\{y'_{n+1} + b'(t_{n+1})[y_{n+1} - y_{n+1}^{(0)}], y_{n+1}\} = 0 \quad (49)$$

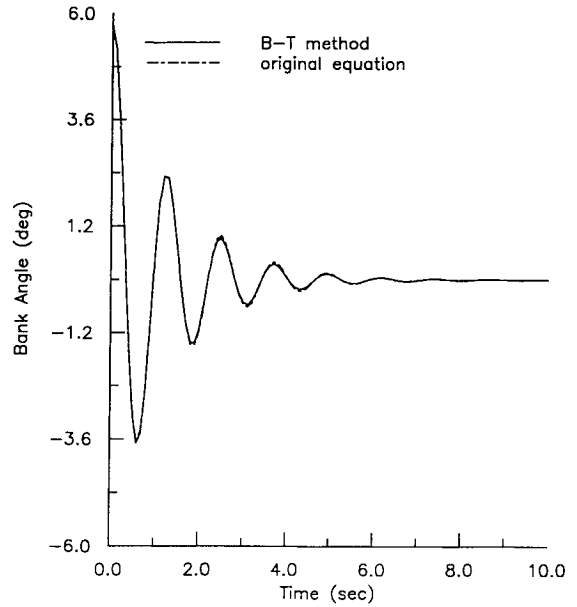


Fig. 5 Bank-angle response based on Beecham-Titchener's method and numerical integration of the original equation (case 2).

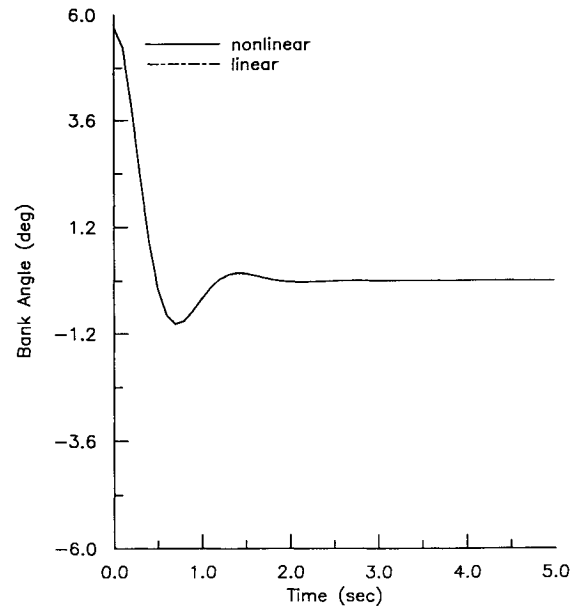


Fig. 6 Bank-angle response to nonlinear and linear control functions (case 7), with the linear function being proportional to p and ϕ only.

which is the corrector equation for y_{n+1} . By using a modified Newton method with an initial approximate value $y_{n+1}^{(0)}$ given by the predictor polynomial, the required solution can be obtained.

System Sensitivity

In a linear theory, system sensitivity is typically investigated by determining the variation in transfer function with respect to the aerodynamic coefficients, or by evaluating singular values of the system matrix. In the present nonlinear theory, it can best be studied by using the frequency and damping that characterize the system output performance.

To determine the system sensitivity, Eqs. (27) are differentiated with respect to the model coefficients c_i ($i = 1, 2, 3, 4$) [see Eq. (3)] to obtain

$$\left[\frac{\partial(d_{11}h_1 + d_{12}h_2)}{\partial\mu} + 2\omega \frac{b_1}{b_3} \right] \frac{\partial\mu}{\partial c_i} + \left[\frac{\partial(d_{11}h_1 + d_{12}h_2)}{\partial\omega} + 2\mu \frac{b_1}{b_3} \right] \frac{\partial\omega}{\partial c_i} = - \frac{\partial(d_{11}h_1 + d_{12}h_2)}{\partial c_i} \quad (50)$$

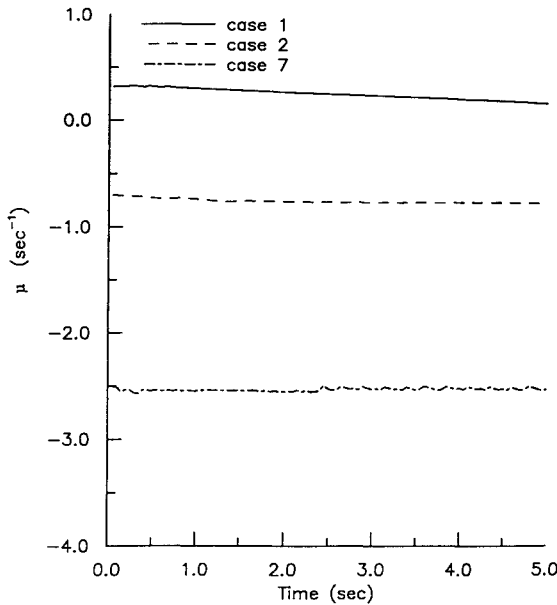


Fig. 7 System damping for different control functions.

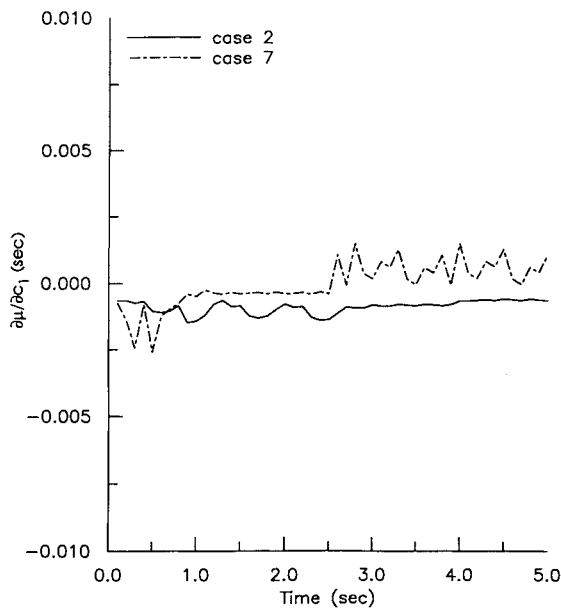


Fig. 8 Sensitivity analysis for $\partial\mu/\partial c_1$.

$$\left[\frac{\partial(d_{21}h_1 + d_{22}h_2)}{\partial\mu} - 2\mu \frac{b_1}{b_3} \right] \frac{\partial\mu}{\partial c_i} + \left[\frac{\partial(d_{21}h_1 + d_{22}h_2)}{\partial\omega} + 2\omega \frac{b_1}{b_3} \right] \frac{\partial\omega}{\partial c_i} = - \frac{\partial(d_{21}h_1 + d_{22}h_2)}{\partial c_i} \quad (51)$$

In Ref. 13, analytic expressions for those partial derivatives appearing in Eqs. (50) and (51) are presented. By solving for $\partial\mu/\partial c_i$ and $\partial\omega/\partial c_i$, system sensitivity can be investigated.

Results

To illustrate the present method, a specific mathematical model for the wing rock of an 80-deg delta wing⁸ will be used. The model was constructed in Ref. 8 by using the test data of Ref. 14. It is described by taking coefficients c_0 to c_4 [Eq. (3)] as follows:

$$c_0 = 0, \quad c_1 = -26.6667 \text{ s}^{-2} \\ c_2 = 0.76485 \text{ s}^{-1}, \quad c_3 = -2.92173 \text{ rad}\cdot\text{s}^{-1}, \quad c_4 = 0$$

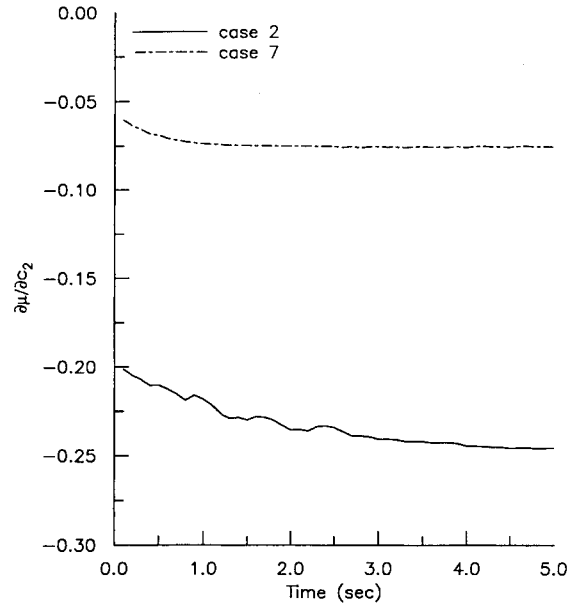


Fig. 9 Sensitivity analysis for $\partial\mu/\partial c_2$.

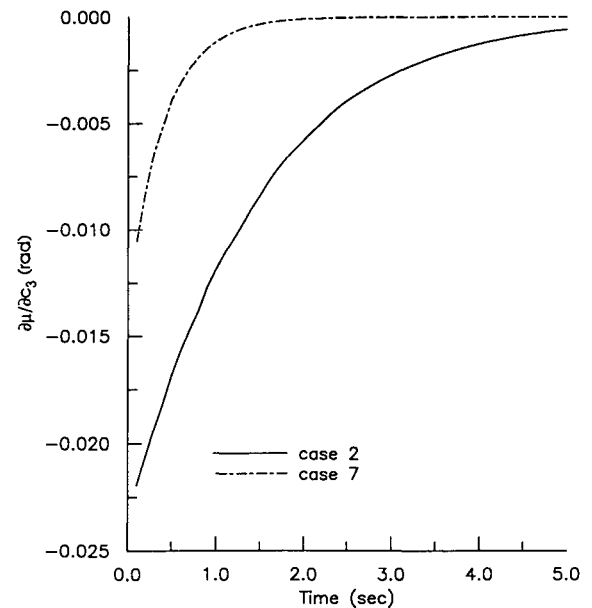
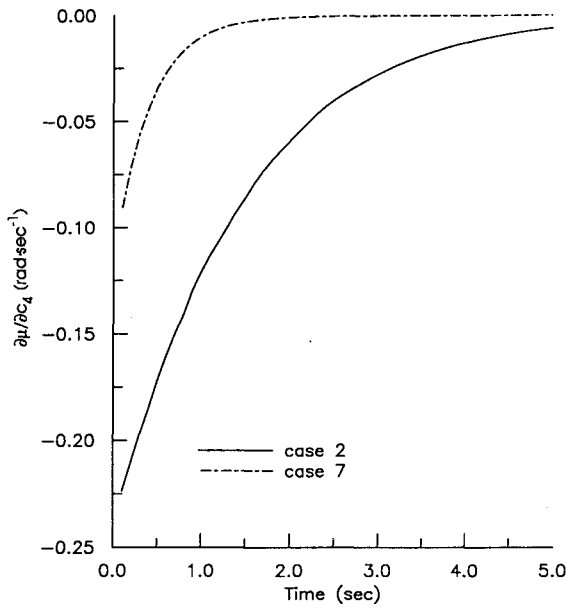


Fig. 10 Sensitivity analysis for $\partial\mu/\partial c_3$.

Table 1 Weighting factors and results for control function

Case	μ_d (s ⁻¹)	ω_d (rad/s)	b_1 (rad-s)	b_2 (rad ² s ⁻¹)	b_3 (s ³)	k_1 (s ⁻²)	k_2 (s ⁻¹)	k_3 (rad ⁻¹ s ⁻²)	k_4 (rad ⁻¹)	k_5 (rad ⁻¹)	k_6 (s ⁻¹)	Error
1	0.32	5.158	0.0	0.0	1	0.0	0.0	0.0	0.0	0.0	0.0	
2	-0.70	5.100	1.71	2.55	1	0.0839	-2.1947	-1.677	0.2401	0.1923	0.0107	5.38E-4
3	-1.50	5.000	7.04	53.95	1	-1.1679	-3.7673	4.167	0.0505	3.0606	2.2322	5.33E-4
4	-1.50	4.900	9.02	0.55	1	0.2441	-3.7100	0.397	-0.0640	-0.252	-1.212	2.40E-4
5	-2.00	4.800	14.31	49.35	1	-0.8575	-4.8538	-11.16	0.7724	-0.176	6.5507	5.80E-4
6	-2.00	4.710	16.02	3.35	1	0.0655	-4.8467	-11.54	0.7450	-0.115	5.8470	4.36E-4
7	-2.50	4.450	25.11	3.39	1	0.0839	-5.7436	0.2517	0.1194	1.7350	1.6832	5.01E-5

Fig. 11 Sensitivity analysis for $\partial\mu/\partial c_4$.

Assume that the initial conditions are given by

$$\phi(0) = 0.1 \text{ rad} = 5.7296 \text{ deg}$$

$$\dot{\phi}(0) = 0.032 \text{ rad/s} = 1.8335 \text{ deg/s}$$

Both the dynamic and control characteristics by the B-T method will be discussed.

Dynamic Characteristics

For this model, Eqs. (20) and (21) become

$$\omega^2 = 26.6667 + \mu^2 - 0.76485\mu + 2.92173a\mu \frac{8}{3\pi} \quad (52a)$$

$$2\mu = 0.76485 - 2.92173a \frac{4}{3\pi} \quad (52b)$$

From Eq. (52b), the following equation for $a(t)$ can be obtained:

$$da/dt = 0.38242a - 0.62a^2$$

which can be integrated with the specified initial conditions to give

$$a(t) = (0.119349e^{0.38242t}) / (1 + 0.19349e^{0.38242t}) \quad (53)$$

As $t \rightarrow \infty$, $a \rightarrow 0.6168 \text{ rad} = 35.34 \text{ deg}$. This agrees with the data very well. Equation (52a) provides the following expression for $\theta(t)$:

$$\frac{d\theta}{dt} = \left(26.6667 + \mu^2 - 0.76485\mu + 2.92173a\mu \frac{8}{3\pi} \right)^{1/2} \quad (54)$$

$$\mu(t) = 0.38242 - 0.62a$$

which can be directly integrated. This semianalytical solution is compared with a direct numerical integration of the original equation [Eqs. (2) and (3) with $u = 0$] by a fourth-order Runge-Kutta scheme in Fig. 1. It is seen that the agreement is very good.

Control Characteristics

By using the B-T method, the weighting factors and optimal control can be computed in accordance with the method described under theoretical development. Application to a linear equation was shown to agree well with the Riccati solution.¹³ The optimal control is given by [see Eqs. (9) and (12)]

$$u(t) = -\frac{a}{2b_3} (\xi_2 \sin \theta + \eta_2 \cos \theta) \quad (55)$$

Note that the solution $u(t)$ is computed only as a function of time. This solution is then expressed as a function of state variables through the least-squares method as follows:

$$u = k_1\phi + k_2p + k_3\phi^2 \operatorname{sgn}(\phi) + k_4p^2 \operatorname{sgn}(p) + k_5p\phi \operatorname{sgn}(\phi) + k_6p\phi \operatorname{sgn}(p) \quad (56)$$

As indicated earlier, the weighting factors in Eq. (4) can be chosen by relating them to the desired system damping and frequency. Results for some choices are presented in Table 1. Case 1 represents the motion without control input. In this case, μ is positive so that it is unstable. For other cases, μ is assumed to have some negative values and ω is arbitrarily varied from the value in case 1. The least-squares error is also presented in the table. It is seen from Table 1 that increasing b_1 leads to an increase in k_2 and hence to more damping. This is also illustrated in Figs. 2 and 3. For case 2, the damping level is lower (-0.7 vs -2.5 for case 7). Therefore, it takes longer for the motion to be suppressed. However, for case 7 the peak required control input is much higher, as shown in Fig. 4. Since b_1 is related to p , it may be concluded that controlling p is more effective in suppressing wing rock.

To illustrate the accuracy of the B-T method, the calculated control function is added to the equation of motion [Eq. (3)] and the latter numerically integrated. The results are compared with the B-T results [Eq. (27)] in Fig. 5. It is seen that the agreement is very good.

As shown in Eq. (56), $u(t)$ depends nonlinearly on the state variables. However, only the linear terms [i.e., the first two terms in Eq. (56)] are important. To illustrate this, the responses based on the full nonlinear control function and the linear terms only are compared in Fig. 6. As can be seen, the results are nearly identical. Physically, this means that the best strategy of suppressing wing rock is to augment the roll damping through the feedback of roll rate.

Results of Sensitivity Analysis

Different controller designs result in different stability margin, i.e., the level of system damping μ above the stability boundary ($\mu = 0$). For the present application, the values of μ

are illustrated in Fig. 7. Again, without control input (case 1), μ is positive and it decreases somewhat as the time increases. With control input (cases 2 and 7), μ stays relatively constant. With a system's controller having been designed, the derivatives $\partial\mu/\partial c_i$ and $\partial\omega/\partial c_i$ ($i = 1, 2, 3, 4$) [see Eqs. (50) and (51)] can be calculated to indicate system sensitivity to small variations in the aerodynamic model. Especially, $\partial\mu/\partial c_i$ may be used to represent the asymptotic stability robustness of the nonlinear system. The results for the μ derivatives are presented in Figs. 8–11. Other derivatives can be found in Ref. 13. It is seen from Fig. 8 that $\partial\mu/\partial c_1$ is small. This is because c_1 represents the natural frequency. On the other hand, c_2 represents the linear damping. It is seen from Fig. 9 that $\partial\mu/\partial c_2$ varies with time because of the nonlinear effect. Since $|\partial\mu/\partial c_2|$ is larger for case 2 (with lower damping), this means the design is more sensitive to c_2 variation.

The nonlinear aerodynamic effect comes mainly from c_3 and c_4 . Since the right-hand sides of Eqs. (50) and (51) are of the form¹³

$$a \cdot G(a, \mu, \omega, b_i, c_i)$$

$\partial\mu/\partial c_3$, $\partial\mu/\partial c_4$, etc., tend to 0 if $a(t) \rightarrow 0$ as $t \rightarrow \infty$. For case 7 (with high damping), these parameters are much smaller than those in case 2 in magnitude and they tend to 0 much faster, as shown in Figs. 10 and 11. In a linear system ($c_3 = c_4 = 0$), μ and ω are both constants. Therefore, $\partial\mu/\partial c_1 = 0$, and $\partial\omega/\partial c_1$, $\partial\mu/\partial c_2$, and $\partial\omega/\partial c_2$ are all constant.

Conclusions

Dynamics and control of wing rock of slender delta wings were investigated through the Beecham-Titchener averaging technique. The optimal control input to suppress wing rock was determined through a Hamiltonian formulation. A specific numerical model of wing rock for an 80-deg delta wing was solved in detail. The numerical results indicated that Beecham-Titchener's technique is accurate in analyzing the dynamic motion and determining the optimal control input. The results also indicated that it was sufficient to use a linear feedback of state variables, such as roll rate, to suppress wing rock. System sensitivity was investigated by determining the variation of system output damping and frequency with aerodynamic model coefficients. Higher sensitivity was obtained for a system with lower damping.

Acknowledgment

This research was supported by the University of Kansas General Research Fund Allocation 3235-20-0038.

References

- ¹Nguyen, L. T., Yip, L., and Chambers, J. R., "Self-Induced Wing Rock of Slender Delta Wings," AIAA Paper 81-1883, Aug. 1981.
- ²Levin, D., and Katz, J., "Dynamic Load Measurements with Delta Wings Undergoing Self-Induced Roll-Oscillations," AIAA Paper 83-1320, June 1983.
- ³Hsu, C., and Lan, C. E., "Theory of Wing Rock," *Journal of Aircraft*, Vol. 22, No. 10, 1985, pp. 920–924.
- ⁴Elzebda, J. M., Nayfeh, A. H., and Mook, D. T., "Development of an Analytical Model of Wing Rock for Slender Delta Wings," *Journal of Aircraft*, Vol. 26, No. 8, 1989, pp. 737–743.
- ⁵Nayfeh, A. H., Elzebda, J. M., and Mook, D. T., "Analytical Study of the Subsonic Wing-Rock Phenomenon for Slender Delta Wings," *Journal of Aircraft*, Vol. 26, No. 9, 1989, pp. 805–809.
- ⁶Beecham, L. J., and Titchener, I. M., "Some Notes on an Approximate Solution for the Free Oscillation Characteristics of Non-Linear Systems Typified by $\ddot{x} + F(x, \dot{x}) = 0$," British Aeronautical Res. Council, Repts. and Memo. No. 3651, London, Aug. 1969.
- ⁷Kokotović, P. V., Khalil, H. K., and O'Reilly, J., *Singular Perturbation Methods in Control: Analysis and Design*, Academic, Orlando, FL, 1986.
- ⁸Baumann, W. T., Herdman, T. O., Stalford, H. L., and Garrett, F. E., "A Volterra Series Submodel Approach to Modelling Nonlinear Aerodynamics Systems," AFWAL-TR-88-3040, Flight Dynamics Lab., Wright-Patterson AFB, OH.
- ⁹Simpson, A., "An Algorithm for Autonomous Non-Linear Dynamical Equations," *Aeronautical Quarterly*, Vol. 28, Aug. 1977, pp. 211–234.
- ¹⁰Bryson, A. E., and Ho, Y. C., *Applied Optimal Control*, Hemisphere, New York, 1975.
- ¹¹Brenan, K. E., et al., *Numerical Solution of Initial-Value Problems in Differential-Algebraic Equations*, Elsevier, New York, 1989.
- ¹²Jackson, K. R., and Sacks-Davis, R., "An Alternative Implementation of Variable Step-Size Multistep Formulas for Stiff ODEs," *ACM Transactions on Mathematical Software*, Vol. 6, 1980, pp. 295–318.
- ¹³Lou, J., and Lan, C. E., "Control of Wing-Rock Motion of Slender Delta Wings," AIAA Paper 91-2886-CP, Aug. 1991.
- ¹⁴Nguyen, L. T., Whipple, D., and Brandon, J. M., "Recent Experiences of Unsteady Aerodynamic Effect on Aircraft Flight Dynamics at High Angle of Attack," Paper No. 29, AGARD CP-386, 1985.